

## Evaluation of Neoadjuvant Chemotherapy Response of Breast Cancer at 3.0T

J.-H. Chen<sup>1,2</sup>, S. Bahri<sup>1</sup>, P. Carpenter<sup>3</sup>, H.-J. Yu<sup>1</sup>, R. Mehta<sup>4</sup>, O. Nalcioglu<sup>1</sup>, and M.-Y. L. Su<sup>1</sup>

<sup>1</sup>Center for Functional Onco-Imaging, UC Irvine, Irvine, CA, United States, <sup>2</sup>China Medical University Hospital, Taichung, Taiwan, <sup>3</sup>Department of Pathology, UC Irvine, Irvine, CA, United States, <sup>4</sup>Department of Medicine, UC Irvine, Irvine, CA, United States

**Background and Purpose:** For locally advanced breast cancer that is inoperable, neoadjuvant chemotherapy (NAC) is the standard of care used to downstage the tumor to render it operable. However, in recent several years NAC has also been extensively used for patients with readily operable breast cancer to facilitate breast conservation surgery. Precise evaluation of the tumor response and residual tumor area following NAC using imaging may provide very helpful information for clinicians and patients to decide the optimal surgical plan. Our previous publication [1] has shown that 1.5T MR failed to detect residual disease presenting as scattered tumor cells or clusters < 2mm. 3.0 T offers a higher SNR and better spatial resolution, and the purpose of this work was to compare the residual breast cancer after NAC measured by 3.0T MRI and the pathological examination.

**Materials and Methods:** In a retrospective review of breast MRI database from March 2007, 33 women who received NAC (N=29) and neoadjuvant hormonal therapy using anastrozole (Arimidex®, N=4), and have pre- and post-treatment MRI were analyzed in this study. The NAC protocol contained sequential Adriamycin (Doxorubicin) and Cyclophosphamide (AC) and taxane-based regimen. HER-2-positive patients also received trastuzumab (Herceptin) and HER-2-negative patients received bevacizumab (Avastin®) with taxane. A definitive surgery was performed following treatment. Using RECIST criteria, the longest dimension of the tumor was determined on the final MRI, by referencing to the pre-treatment and all prior F/U studies. Complete clinical response (CCR) was diagnosed when no enhancement or faint enhancement equal to the background normal breast tissue was noted in the previous lesion site in MRI. For all cases, the pathological examination of the residual disease was performed by a pathologist using consistent criteria. If a solid mass was found, the largest dimension of the tumor was given. If scattered cells or cell clusters were found, the size of the largest foci and the extent of tissue region where the residual cancer cells were present were specified. Pathological complete response (pCR) was defined as no residual invasive cancer cells, with or without DCIS.

**Results:** Of the 33 cases, 20 were mass lesions (6 multiple masses) and 13 were non-mass enhancement. Ten patients had Her-2 positive cancers and 23 had Her-2 negative cancers. MRI showed 10 patients with complete clinical response (without visible contrast enhancements) and 23 with residual cancers. Pathological findings showed 10 pCR (6 Her-2 positive and 4 Her-2 negative). MRI had false negative diagnosis in two non-mass enhancement lesions, in which pathology showed extensive scattered small cancer foci in 3 cm and 14 cm (Figure 1) areas respectively. MRI showed false positive diagnoses in 4 patients, three with mass lesions and one with non-mass lesion. In these 4 patients, low but visible enhancement was noted in MRI whereas only DCIS was noted in pathology, thus considered as pCR cases. MRI had 19 true positive diagnoses and 8 true negative diagnoses. For the correlation of residual tumor size between MRI and pathology, non-mass lesions had wider size discrepancy than mass lesions (0.9-14cm vs. 0-3cm) (two case examples shown in Figure 1). Overall, mass lesions showed much higher correlation coefficient than non-mass enhancement lesions ( $r=0.92$  vs.  $r=0.32$ ). One mass lesion had 3cm discrepancy between MRI and pathology due to its speculated margin and being unable to be correctly measured in MR. Figure 2 showed the correlation of MRI and pathology for mass lesions.

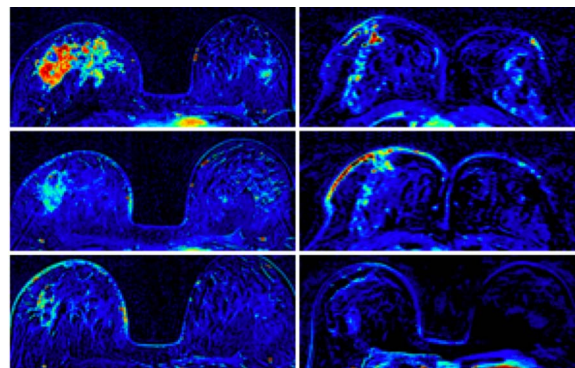


**Fig.1:** Response of two non-mass lesions at baseline (top), during NAC (middle), and after NAC (bottom). Left column: a 9.8 cm non-mass lesion prior to NAC, reduced to 5.6 cm and then to 3 cm after NAC. Pathology showed scattered cancer nests in a 10 cm area. Right column: a linear non-mass enhancement lesion showed gradual reduction of enhancement down to invisible at the last MRI. Pathology, however, showed residual cancer in a 14 cm area.

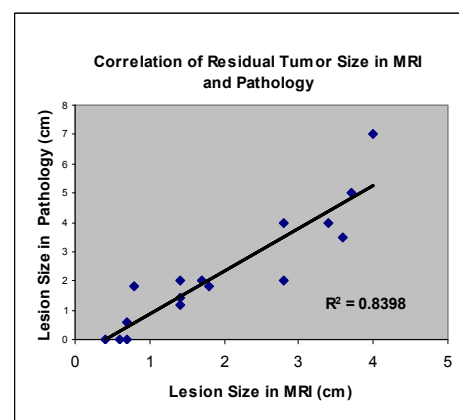


**Fig.2:** In mass type lesions, the sizes of the residual tumor measured by MRI and pathology after NAC are highly correlated.

**Conclusions:** The results analyzed from 3.0 T were consistent with our previous findings using 1.5T with a lower spatial resolution, suggesting that the limitation of MRI in diagnosis of post-NAC cancer cannot be improved with a higher SNR or a higher spatial resolution. Our current protocol at 3.0 T still could not detect residual tumor presenting as scattered cells or small foci, which often occurs in non-mass-like lesions. These types of invasive cancer cells do not need angiogenesis to survive, and if so, they will not show contrast enhancements. Therefore, even if the spatial resolution of MRI can be further improved down to the mm range, it is still not possible to detect them. Caution should be taken for the surgical planning of non-mass enhancement lesions based on MRI findings. Nevertheless, it is commonly agreed that the subsequent radiation therapy will very likely kill these scattered cells. Particularly given the current debate about the value of additional true positive lesions detected by pre-operative MRI, it may be possible that accurate detection of minimal diseases (such as the scattered cells reported here) is not clinically significant. Further research is warranted.

**Reference:** [1] Chen et al. Cancer. 2008;112:17-26

**Acknowledgement:** This study was supported in part by NIH/NCI R01 CA90437, CA127927